Linear quadratic regulator Based Control Algorithm Optimized by Particle Swarm Optimization for Seismically Excited Buildings

Houria Amamra[1], Othmen Benmekki[1] and Oualid Limam[1]

[1] *Department of civil engineering, ENIT, University of Elmanar, Tunis, Tunisia*

e-mail: amamra.houria@enit.utm.tn, othmen.benmekki@enit.rnu.tn, oualid.limam@enit.rnu.tn

Abstract

In the last decades, a lot of different seismic semi-active control algorithms have been proposed, which are generally based on traditional control applications. In this paper we develop a new control algorithm for multi degree of freedom MDOF structures based in Linear quadratic regulator control optimized by Particle swarm optimization (PSO) algorithm. This algorithm uses LQR's direct approach for stability analysis in design of feedback controller. The PSO algorithm provides the optimal parameters of Linear quadratic regulator function candidate, which minimize the evaluation criteria function of the states of the system. Numerical simulations using three story frame structure modeled as shear building structure subjected to earthquake excitations have been performed to evaluate the effectiveness of the proposed algorithm.

Keywords: Seismic semi-active control, multi degree of freedom MDOF, Linear quadratic regulator, stability, Particle swarm optimization (PSO), Optimization, Numerical simulation.

1 Introduction and Preliminaries

Buildings installed with control systems may still suffer from a certain level of damage under an earthquake event [2, 11]. Such damage requires different control forces to mitigate seismic response, as compared to undamaged ones, when subjected to next earthquake event. As a result, control systems for buildings require initial input data from damage detection technologies.
There has been a large amount of research effort devoted to the theoretical and practical development of structural control, especially in countries where earthquakes are active [14, 5].
Structural control can be applied to mitigate the vibration amplitudes by using appropriate devices and control techniques [9]. The key element in successful use of these devices and techniques is an effective control lgorithm to compute loads to be applied to the structure, and it demonstrated that the performance of the controlled system is highly dependent on the choice of algorithm [10] . An effective control algorithm has to be robust and functional under various dynamic

conditions. Various control algorithms have been proposed, and based in different optimization procedures including linear quadratic regulator (LQR) [1, 3].

The LQR control is among the well-known optimal algorithms mainly due to its simplicity and ease of implementation. Then, it is regarded as a baseline in modern control theory [3]. Even though it can be used to reduce vibrations, it suffers from a number of shortcomings, such as being susceptible to parameters uncertainty and modelling error. Another drawback is the difficulty to study the stability of controlled structures [3]. However, for the practical application of an active control method to civil engineering structures, the problem of stability and robustness is one of the major issues and it has been examined in several studies [13]. Design of a stable and robust controller is possible by using (LQR) based PSO control.

The concept of particle swarm optimization (PSO) was originally introduced by Kennedy and Eberhart in 1995 [8] as a technique for individual improvement through population cooperation and competition, which is based on the simulation of a simplified social model, such as bird flocking, fish schooling and the swarm theory. Its mechanism enhances and adapts to the global and local exploration. Some of the key advantages are that this method does not require the calculation of derivatives, that the knowledge of good solutions is retained by all particles, and that these particles in the swarm share information between them PSO is less sensitive to the nature of the objective function, can be used for stochastic objective functions and can easily escape from local minima. Concerning its implementation, PSO can easily be programmed, has few parameters to regulate, and the assessment of the optimum is independent of the initial solution. Nowadays, PSO has gained much attention and wide application in various fields. The basic PSO algorithm consists of three steps, generating particles, positions and velocities, velocity update, and position update. Here, a particle refers to a point in the design space that changes its position from one move (iteration) to another based on velocity updates [4].

In this paper, a Linear quadratic regulator (LQR) based PSO seismic control algorithm is developed for a multi degree of freedom (MDOF) equipped with an MR damping, civil engineering structures subjected to a seismic ground motion. It is important to note that for its application, this proposed control algorithm needs to know the mass, damping and stifness of the structure. To evaluate the effectiveness of the proposed algorithm, numerical simulations on controlled and uncontrolled seismic behavior of a multi story shear building structure have been conducted. The structure analysis and control design are carried out using a computer program developed with MATLAB.

2 Mathematical modelling of problem

Let's start out with the equation of motion for a system with multi degree of freedom (MDOF) controlled with a single MR damper, subjected to a seismic ground excitation $\ddot{x}_g(t)$.

$$M\ddot{x} + C\dot{x} + Kx = -F_u - M\ddot{x}_g$$

where $x, \dot{x}, \ddot{x}$ are the vectors of the displacements, velocity, and acceleration respectively of the floors of the structure. M, C, and K are mass, damping and stifness matrix coefficients respectively, F_u is the vector of control forces.

This equation can be written in state-space form as

$$\dot{Z}(t) = AZ(t) + B_u u(t) + B_r \ddot{x}_g(t).$$

Where

$$A = \begin{pmatrix} [0] & [I] \\ -[M]^{-1}[K] & -[M]^{-1}[C] \end{pmatrix}$$

, Z is the state vector, and

$$B_u = \begin{pmatrix} [0] \\ -[M]^{-1} \end{pmatrix}$$

and

$B_r = ([0], [I])$

3 Semi-active damper modelling

Controllable fluid dampers have fluids whose properties can be influenced by the presence of a magnetic or electric field. [19, 21] The MR damper can be described by a dynamical model of a damper with a MR fluid, equivalent to two dampers in parallel: a passive damper and a dynamic damper in the sense of a variable damping coefficient. The sum of the two components yields the MR total damping force f_{MR}

$$f_{MR} = f_p(x, \dot{x}) + f_I(x, \dot{x}, I)$$

$$f_p = k_e x + c_e \dot{x}$$

$$f_I = y_f I.g(\dot{x}, x)$$

where $x = z_{def}$, $\dot{x} = \dot{z}_{def}$, f_p is the passive damping force, I is the electric current through the coil, f_I is the damping force due to I, k_e is the passive stiffness coefficient, c_e is the passive damping coefficient, y_f is the yield point coefficient of f_I , $g(.)$ is a nonlinear function. This structure is used to study the action of the electric current on the MR damper force. [18]

A variety of approaches have been proposed in the literature for the control of semi-active devices. Subsequently, a selection of these approaches will be presented and evaluated for a numerical example. In developing the control laws, note that

i) the control voltage is restricted to the range $v \in (0, V_{max})$, and

ii) for a fixed set of states, the magnitude of the applied force $|f|$ increases when v increases, and decreases when v decreases [7].

The behavior of the MR damper used in this case study is given by [20]

$$\left\{\begin{array}{c} F = c_0\dot{x} + \alpha z \\ \dot{z} = -\delta|\dot{x}|z|z|^{n-1} - \beta\dot{x}|z|^n + A\dot{x} \\ \alpha = \alpha_a + \alpha_b u \\ c_0 = c_{0a} + c_{0b}u \\ \dot{u} = -\eta(u - u_V) \end{array}\right\}$$

Where F is the force generated by the damper, u is the command signal, u_V is the command voltage, $\dot{x}$ is the velocity of the structure.

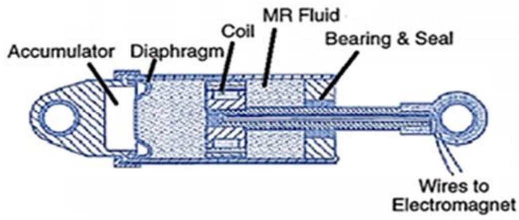

(a)

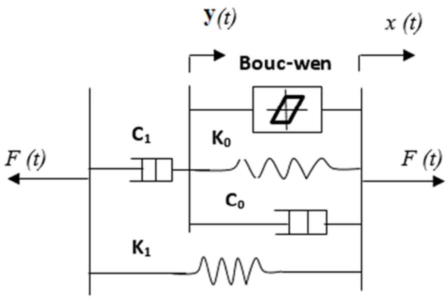

(b)

Figure 1. Schematic diagram and simple mechanical model of an MR damper.

(a): Small scale MR fluid damper; (b): the phenomenological model for the MR damper.

4 Proportional-Integral-Derivative Control (PID)

A PID controller works on the basis of calculating appropriate control actions based on a calculated feedback error. For negative feedback control system, the error defined as the difference of the output signal to a desired reference signal. In order to assure the correct desired output forces from both dampers, an internal negative feedback loop has been closed, using a PID controller, the tuning of which has been obtained by means of PSO algorithm. The damper will be mounted at the base of the structure, their main objective being the decoupling of the sructure from the ground motion. The PID controller has been chosen for control of the damper's output force in order to construct a control loop that will be used as an internal loop in a cascade configuration with advanced control algorithms for the structure displacement. As opposed to the conventional control algorithms (mainly PID and variants of on-off laws), advanced control includes algorithms such as state control, adaptive control, intelligent control system.

5 The proposed algorithm LQR with PID based PSO control

This section brings forth the practical aspect of using particle swarm optimization (PSO) in aiding PID (Proportional - Integral- Derivative) control design for real world industrial processes.

5.1 Particle Swarm Optimization

Particle swarm optimization (PSO) is a population-based optimization method, first proposed by Kennedy and Eberhart in 1995, inspired by social behavior of bird flocking or fish schooling. The PSO as an optimization tool provides a population-based search procedure in which individuals called particles change their position (state) with time. In a PSO system, particles fly around in a multidimensional search space. During flight, each particle adjusts its position according to its own experience (This value is called p best), and according to the experience of a neighboring particle (This value is called g best), made use of the best position encountered by itself and its neighbor (Fig. 2).

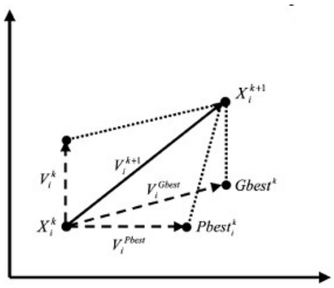

Figure 2. Concept of serching point by PSO

This modification can be represented by the concept of velocity. Velocity of each agent can be modified by the following equation:

$$v_{k+1} = \omega v_k + c_1 r_1 * (pbest - x^k) + c_2 r_2 * (gbest - x^k)$$

Using the above equation, a certain velocity, which gradually gets close to p best and g best can be calculated. The current position (searching point in the solution space) can be modified by the following equation

$$x^{(k+1)} = x^k + v_{k+1},\ k = 1, 2, ..., n.$$

Where x^k is current searching point, $x^{(k+1)}$ is modified searching point, v_k is current velocity, v_{k+1} is modified velocity of agent v_{pbest} is velocity based on p best, v_{gbest} is velocity based on g best, n is number of particles in a group, m is number of members in a particle, $pbest_i$ is p best of agent k, $gbest_i$ is g best of the group, ω is weight function for velocity of agent k , c_i is weight coefficients for each term.
- c_1 and c_2 are two positive constants.
- r_1 and r_2 are two randomly generated numbers with a range of $[0, 1]$.
- ω is the inertia weight and it is defined as a function of iteration index k as follows:

$$\omega_k = \omega_{max} - (\frac{\omega_{max} - \omega_{min}}{Max.Iter}) * k.$$

Where Max.Iter is maximum number of iterations and k the current number of iterations. To insure uniform velocity through all dimensions, the maximum velocity is as $v_{max} = \frac{x_{max}-x_{min}}{N}$, where N is a chosen number of iterations.

5.2 PID controlled with PSO

For the purpose of this case study, a base isolation system is considered for a multiple story building. The damper is mounted in the base of the structure which is controlled via an LQR law on the outer loop of a cascaded control system. The design on the LQR law, the building model and its state space representation are described in [16]. In order to maintain the computational requirements of the control system to a minimum, a PID controller is chosen to be designed using PSO for the inner loop containing the damper. This configuration is presented in [17], page 111, Figure 20, (here see Fig. Configuration),

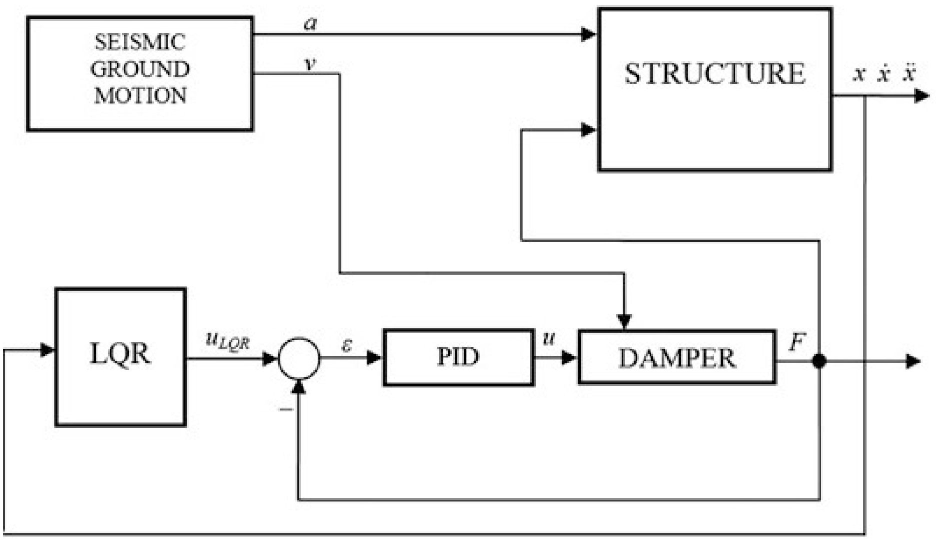

Fig. Configuration, Cascaded control structure for building equipped with MR damper

where x is the displacement of the structure, $\dot{x}$ and $\ddot{x}$ are the velocity and acceleration of the structure, respectively, F is the control force as damper output; u_{LQR} is the desired control force, u is the command signal, ϵ is the control deviation of the inner loop; a and v are the ground acceleration and velocity, respectively.

The PID damper controller is chosen to be of the form

$$u(t) = Kr.\epsilon(t) + Ki.\int_0^t \epsilon(x)dx + Kd.\frac{d\epsilon(t)}{dt}$$

where $u(t)$ is the command, $\epsilon(t)$ is the control deviation, Kr is the PID proportional gain, Ki the integral gain, and Kd the derivative gain.

6 Numerical example and simulation

The Linear quadratic regulator LQR control method is applied to minimize steady state error and multiple overshoot. This control algorithm has been developed for a three degree of freedom structure and LQR without damper inner-loop is used for results comparison. The behavior of this structure is analyzed for the cases of uncontrolled, LQR based control and this proposed LQR with damper PSO-PID inner-loop control. The structure considered is a three story shear building. The structural mass and stiffness have been concentrated in floor and columns respectively. The parameters of this structure are

$$M = \begin{pmatrix} 98.3 & 0 & 0 \\ 0 & 98.3 & 0 \\ 0 & 0 & 98.3 \end{pmatrix} [kg]$$

$$C = \begin{pmatrix} 175 & -50 & 0 \\ -50 & 175 & -50 \\ 0 & -50 & 50 \end{pmatrix} [Ns/m]$$

$$K = 10^5 \begin{pmatrix} 12 & -6.84 & 0 \\ -6.84 & 13.7 & -6.84 \\ 0 & -6.84 & 6.84 \end{pmatrix} [N/m]$$

$$C_{md} = \begin{pmatrix} 8.64 & 0.51 & 0.03 \\ 0.51 & 8.56 & 0.54 \\ 0.30 & 0.54 & 9.08 \end{pmatrix} [Ns/m]$$

The MR damper model parameters are chosen values as follows
$c_{0a} = 0.0064N_s/cm$, $c_{0b} = 0.0052N_s/cmV$, $a_a = 8.66N/cm$, $a_b = 8.86N/cmV$, $\delta = 300cm^{-2}$, $\beta = 300cm^{-2}$, $A = 120, n = 2$ and $\eta = 80s^{-1}$.

The MR damper is rigidly connected between the ground and the structure, as shown in Fig. 3.

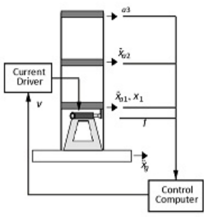

Figure 3. Diagram of MR Damper Implementation

The simulations were carried out under the historic earthquake excitations with different frequency content:

- El Centro 1940 accelerogram with peak ground acceleration (PGA) of 0.2983 m/s^2.
- Northridge 1994 accelerogram with peak ground acceleration (PGA) of 8.4758 m/s^2.
- Chi-Chi 1999 accelerogram with peak ground acceleration (PGA) of 7.9823 m/s^2.
- San Fernando 1971 accelerogram with peak ground acceleration (PGA) of 2.6544 m/s^2.

- Loma Prieta 1989 accelerogram with peak ground acceleration (PGA) of 4.7975 m/s^2.

These records have been extensively used in various research studies and practical control applications throughout the world. Their accelerograms are shown in Figure 4.

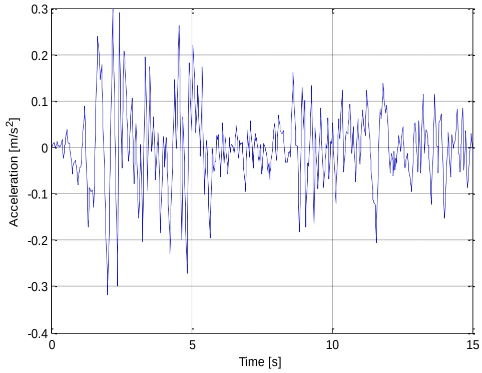

(a) El Centro 1940 ground motion

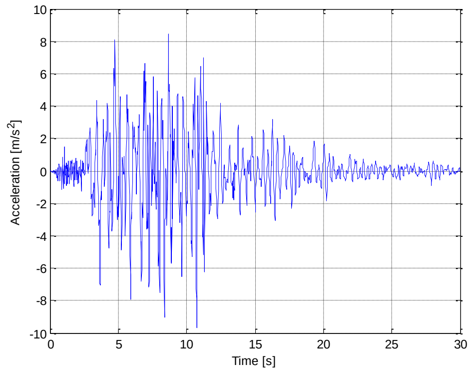

(b) Northridge 1994 ground motion

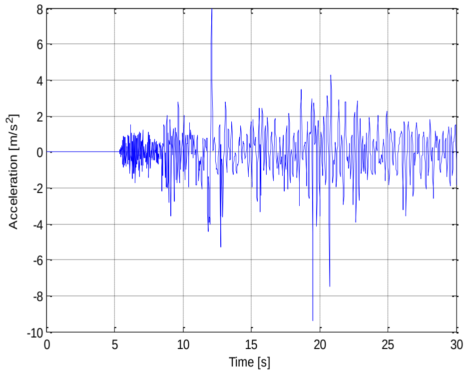

(c) Chi-Chi 1999 ground motion

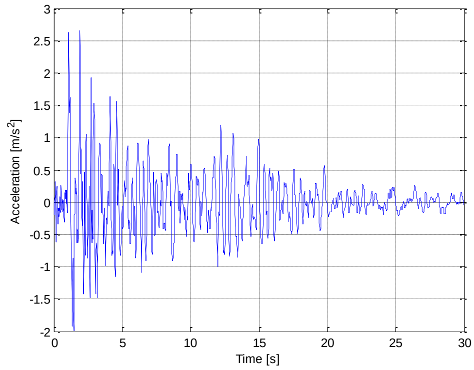

(d) San Fernando 1971 ground motion

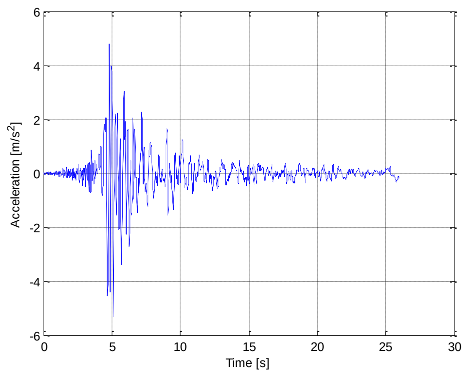

(e) Loma Prieta 1989

Fig. 4. Excitation accelerograms

To evaluate the control algorithm in terms of reduction of peak responses, the following evaluation criteria adopted from [6, 15] are considered:
1. Story displacement ratio

$$J_1 = \frac{max|y_c|}{max|y_u|}.$$

Where y_c is the controlled story displacement, y_u Uncontrolled story displacement.

2. Story acceleration ratio

$$J_2 = \frac{max|\ddot{y}_c|}{max|\ddot{y}_u|}.$$

Where $\ddot{y}_c$ Controlled story acceleration, $\ddot{y}_u$ Uncontrolled story acceleration.

3. Root mean square (RMS) story displacement ratio

$$J_3 = \frac{\vec{y_c}}{\vec{y_u}} = \frac{std(y_c)}{std(y_u)},$$

we can find $\vec{y_c}$ and $\vec{y_u}$ from

$$\vec{y} = std(y) * \sqrt{\frac{T_s}{T_f}}$$

Where T_s is the sampling time, T_f is the total excitation duration, and std is the standard deviation.

4. Root mean square (RMS) story acceleration ratio

$$J_4 = \frac{\vec{\ddot{y}_c}}{\vec{\ddot{y}_u}} = \frac{std(\ddot{y}_c)}{std(\ddot{y}_u)},$$

we can find $\vec{\ddot{y}_c}$ and $\vec{\ddot{y}_u}$ from

$$\vec{\ddot{y}} = std(\ddot{y}) * \sqrt{\frac{T_s}{T_f}}$$

Tab. 1. Maximum displacement and acceleration

	Displacement(cm)	Velocity(m/s)	Acceleration (m/s²)
El Centro 1940			
Uncontrolled	0.4308	0.1457	8.2252
LQR without damper inner loop	0.4610	0.0980	6.2379
LQR with damper PID-PSO inner loop	0.2130	0.1227	5.1391
Northridge 1994			
Uncontrolled	3.6063	1.1583	40.8361
LQR without damper inner loop	1.6144	0.4583	19.8271
LQR with damper PID-PSO inner loop	1.0662	0.6527	14.7950
Chi-Chi 1999			
Uncontrolled	1.4163	0.4592	16.7604
LQR without damper inner loop	1.1831	0.3781	14.1103
LQR with damper PID-PSO inner loop	0.7256	0.3954	17.9557
San Fernando 1971			
Uncontrolled	0.4455	0.1433	4.6670
LQR without damper inner loop	0.4825	0.0969	4.8426
LQR with damper PID-PSO inner loop	0.2569	0.1322	2.5088
Loma Prieta 1989			
Uncontrolled	1.3669	0.4248	14.0908
LQR without damper inner loop	0.9971	0.2930	9.3197
LQR with damper PID-PSO inner loop	0.8426	0.4859	8.6965

Tab. 2. Responses Ratios (evaluation criteria)

	J1	J2	J3	J4
El Centro 1940				
LQR without damper inner loop	1.0702	0.7583	0.4953	0.5211
LQR with damper PID-PSO inner loop	0.4945	0.6248	0.2627	0.5241
Northridge 1994				
LQR without damper inner loop	0.4476	0.4855	0.3108	0.2946
LQR with damper PID-PSO inner loop	0.2956	0.3623	0.2273	0.2110
Chi-Chi 1999				
LQR without damper inner loop	0.8353	0.8418	0.7509	0.7326
LQR with damper PID-PSO inner loop	0.5122	1.0713	0.4930	1.0458
San Fernando 1971				
LQR without damper inner loop	1.0830	1.0376	0.6357	0.5174
LQR with damper PID-PSO inner loop	0.5766	0.5375	0.3725	0.3123
Loma Prieta 1989				
LQR without damper inner loop	0.7294	0.6614	0.5830	0.5423
LQR with damper PID-PSO inner loop	0.6164	0.6171	0.4614	0.4377

Results

The first table provides the peak responses of the structure for the cases of uncontrolled, LQR without damper inner-loop control and proposed LQR with damper PID-PSO inner-loop control for the considered ground motions. It is noted from this table, that the reduction in the peak story displacement without control compared with the LQR without damper inner-loop control is 55.23 %, 16.46 % and 27.05 % under Northridge, Chi-Chi and Loma Prieta and close to the test limit under El Centro and San Fernando respectively, and the corresponding reductions compared with the proposed LQR with damper PID-PSO inner-loop are 50.55 %, 70.44%, 48.77%, 42.33% and 61.66%. Similar trends are observed for peak acceleration and velocity. Table 2 summarizes the comparison of evaluation criteria between the LQR without damper inner-loop control case and proposed LQR with damper PID-PSO inner-loop control. The results indicate that the proposed LQR with damper PID-PSO inner-loop control outperforms the LQR without damper inner-loop control under all considered ground motions. The reduction ratios for displacement, acceleration, RMS displacement, and RMS acceleration are much smaller with the proposed LQR with damper PID-PSO inner-loop control. For instance, under the San Fernando record, the reduction ratios are 46.76%, 48.20%, 55.39%, and 39.64% for displacement, acceleration, RMS displacement, and RMS acceleration, respectively. The corresponding reduction ratios under Northridge, Chi-Chi, and El Centro records are also reported.
Responses of the structure for the cases of uncontrolled, LQR without damper inner-loop control and proposed LQR with damper PID-PSO inner-loop control, in terms of displacement, acceleration and Velocity, under the five considered earthquake excitations are depicted in Figures 5, 6 and 7. The figures indicate response reduction for both control algorithms, however it is more significant in case of the proposed LQR with damper PID-PSO inner-loop control for the five earthquake records.

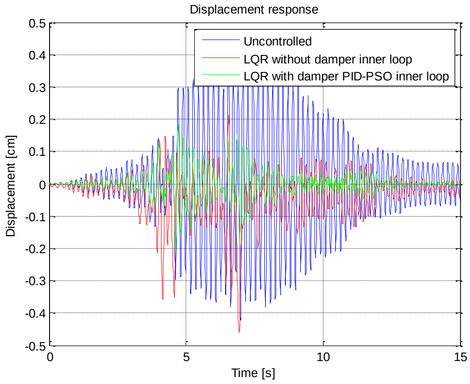

(a) El Centro

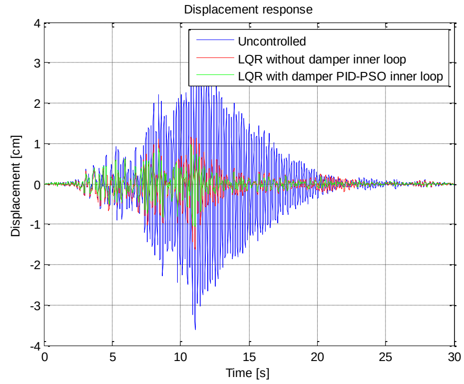

(b) Northridge

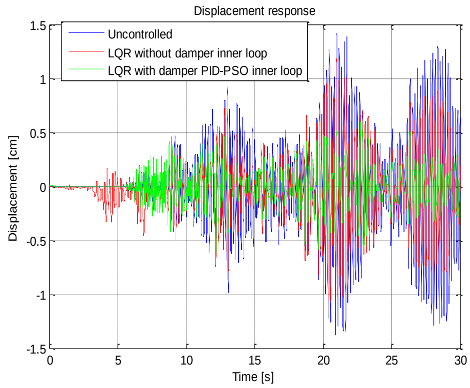

(c) Chi-Chi

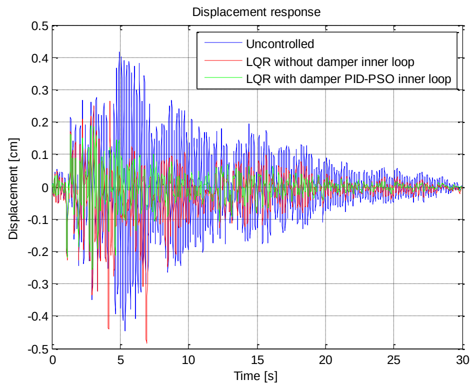

(d) San Fernando

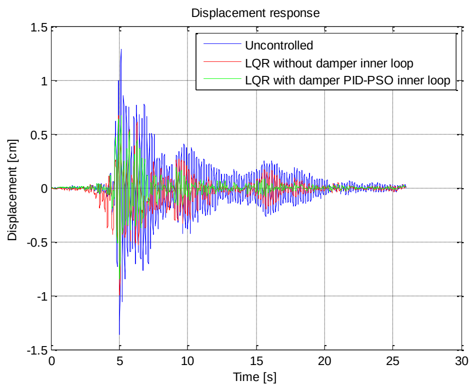

(e) Loma Prieta 1989

Fig. 5. Story displacement of the building under Earthquake Signals

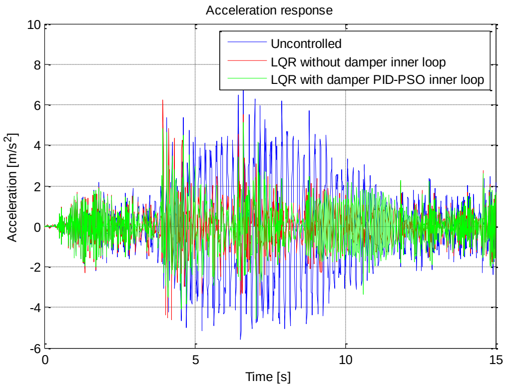

(a) El Centro

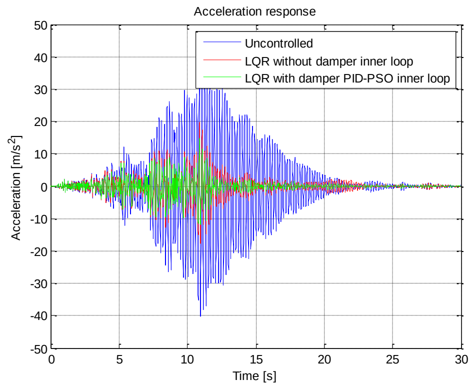

(b) Northridge

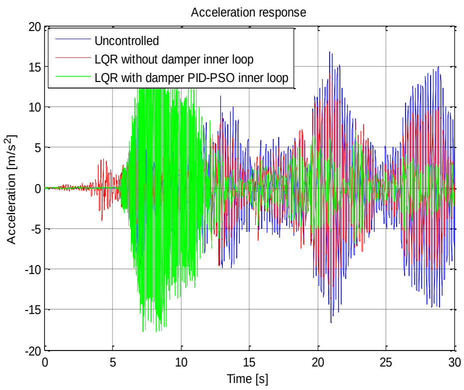

(c) Chi-Chi

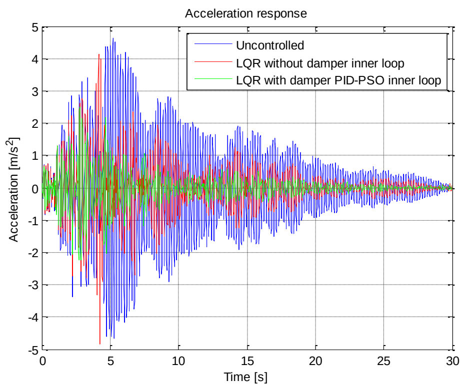

(d) San Fernando

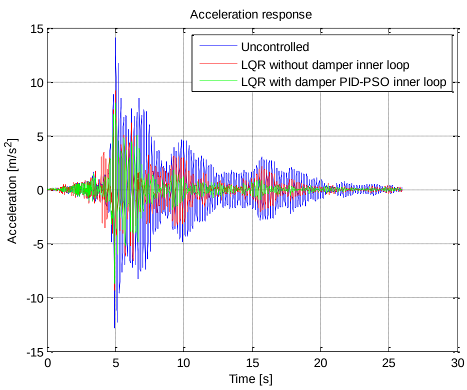

(e) Loma Prieta 1989

Fig. 6. Story Acceleration of the building under Earthquake Signals

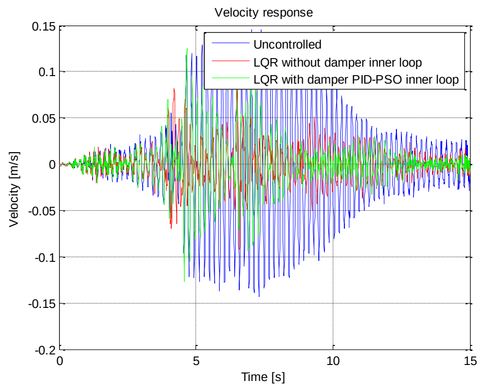

(a) El Centro

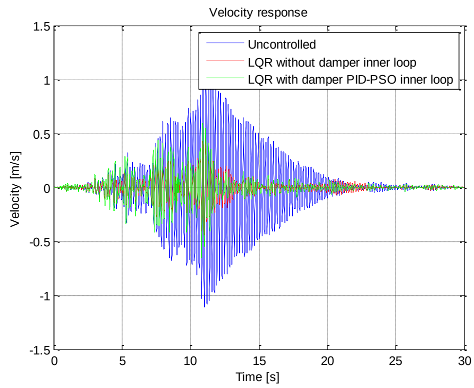

(b) Northridge

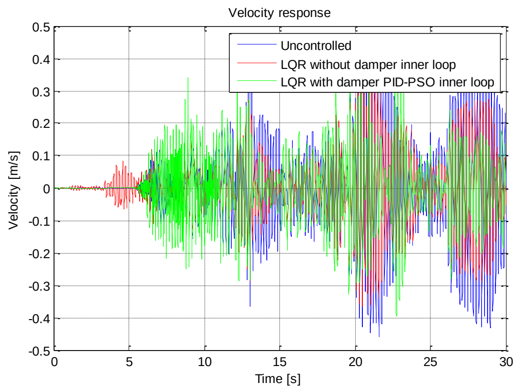

(c) Chi-Chi

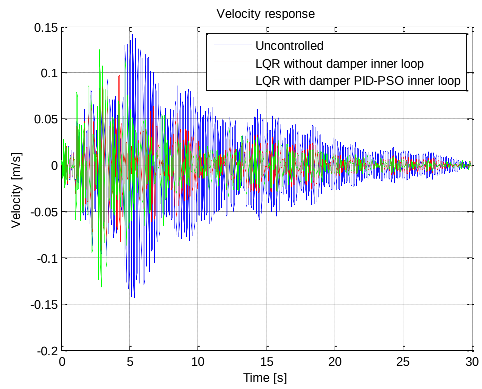

(d) San Fernando

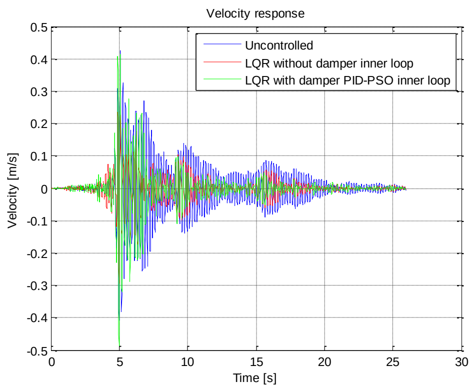

(e) Loma Prieta 1989

Fig. 7. Story Velocity of the building under Earthquake Signals

Figures 8 and 9 illustrate the voltage and control force under Earthquake Signals.

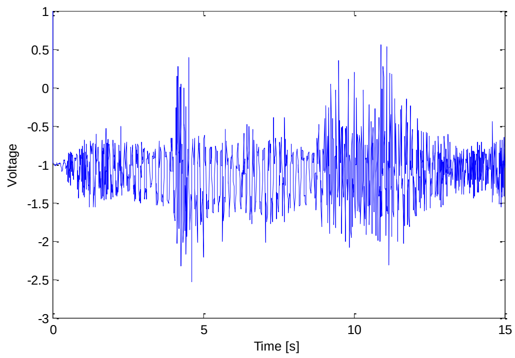

(a) El Centro

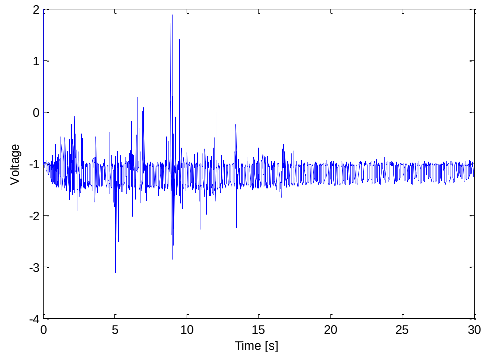

(b) Northridge

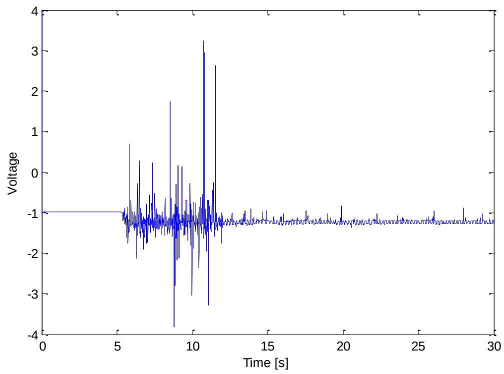

(c) Chi-Chi

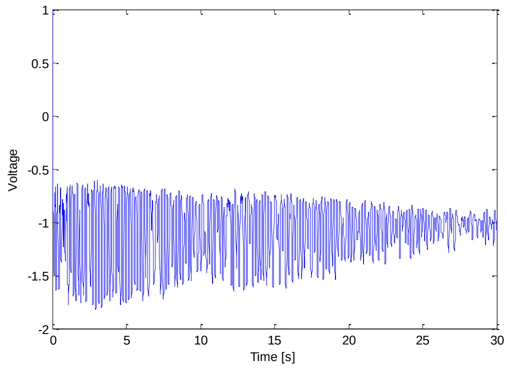

(d) San Fernando

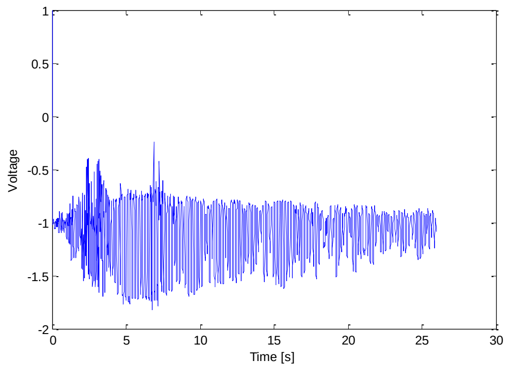

(e) Loma Prieta 1989

Fig. 8. MR Damper control voltage under Earthquake Signals

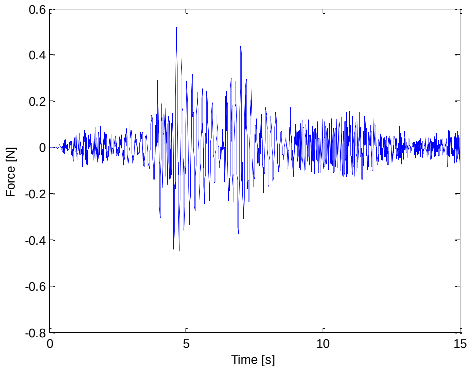

(a) El Centro

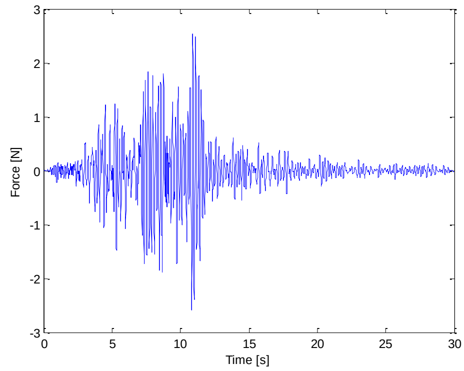

(b) Northridge

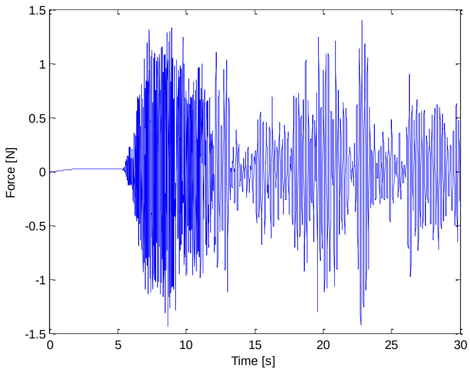

(c) Chi-Chi

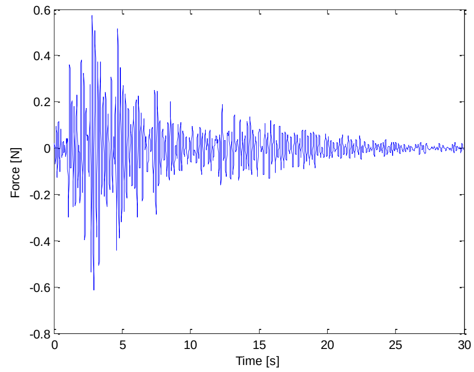

(d) San Fernando

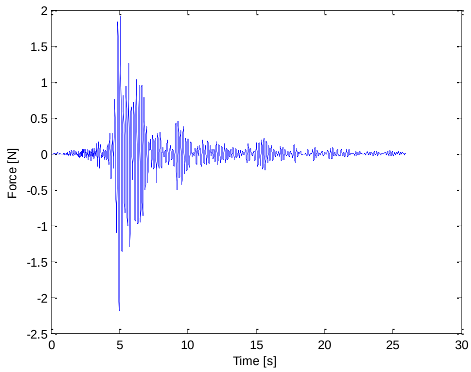

(e) Loma Prieta 1989

Fig. 9. MR Damper control force under Earthquake Signals

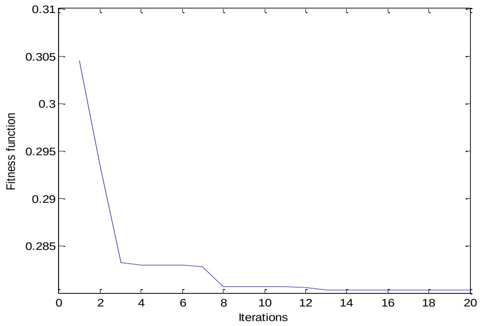

(a) El Centro

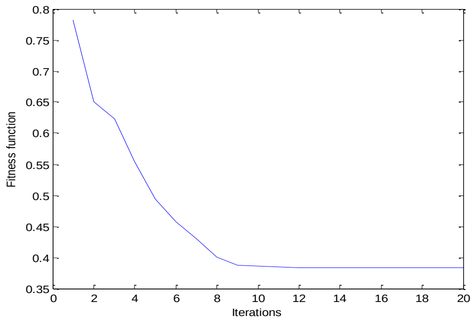

(b) Northridge

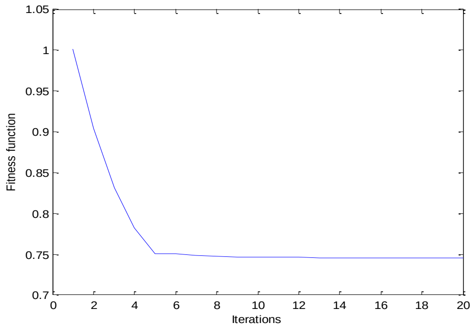

(c) Chi-Chi

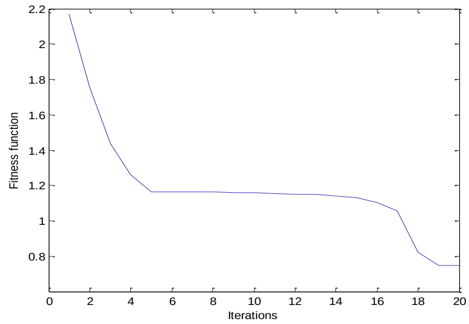

(d) San Fernando

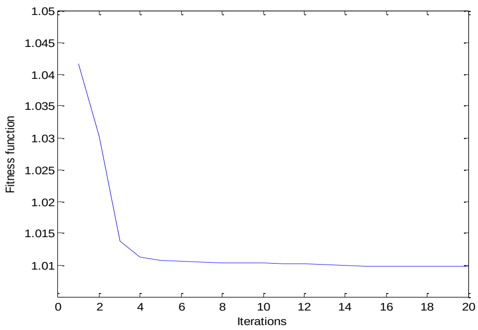

(e) Loma Prieta 1989

Fig. 6. Convergence of fitness value

Fig. 6 illustrates the convergence behavior of the fitness value over iterations for different seismic events: El Centro Northridge, Chi-Chi, and San Fernando. The convergence analysis shows that the PSO algorithm effectively minimizes th fitness value for all the seismic events. This indicates that the PSO algorithm is well-suited for optimizing the LQR controlle with the inner loop PID-PSO damper for seismic control of structures. These results demonstrate the potential of PSO as a efficient optimization technique for the design of seismic control systems.

7 Conclusions

In this study, a new control algorithm based in LQR with damper PID-PSO inner-loop stability theory is proposed for MDOF building structures under seismic loading. For its application this proposed control algorithm needs to know the mass, damping and stiffness of the structure. The performance of this algorithm is demonstrated by numerical simulations on a multi stories shear building structure subjected to five historical ground motions, El Centro 1940, Northridge 1994, Chi-Chi 1999, San Fernando 1971 and Loma Prieta 1989 which still used in research studies and practical control applications. Simulation results and the evaluation criteria show the effectiveness of the proposed LQR with damper PID-PSO inner-loop controller in reducing displacement and acceleration considerably. Further reduction in velocity is also obtained. Another advantage of this method is that the stability of the structure can be verified without solving the dynamic equation explicitly.

References

[1] Aldemir Ü, Bakioglu M, Semi active control of earthquake-excited structures, Turkish Journal of Engineering and Environmental Sciences, 24, (2000), 237-246.

[2] Amini F., Mohajeri S. A., and Javanbakht M., Semi-active control of isolated and damaged structures using online damage detection, Smart Materials and Structures, vol. 24, p. 105002, 2015.

[3] Arfiadi Y, Hadi M N S, Continuous bounded controllers for active control of structures, Computer and Structures, 84(12), (2006), 798-807, DOI 10.1016/j.compstruc.2006.01.001.

[4] Azraai R. et al., Parametric optimization of magneto-rheological fluid damper using particle swarm optimization, International Journal of Automotive and Mechanical Engineering, June 2015 DOI: 10.15282/ijame.11.2015.37.0218.

[5] Datta T K, A state-of-the-art review on active control of structures, ISET Journal of Earthquake Technology, 40(1), (2003), 1-17.

[6] Djajakesukma SL, Samali B, Nguyen H, Study of A semi-active stiffness damper under various earthquake inputs, Earthquake Engineering and Structural dynamics, 31, (2002), 1757-1776, DOI 10.1002/eqe.181.

[7] Dykeand S.J., Spencer Jr. B.F. , A Comparison of Semi-Active Control Strategies for the MR Damper, Proceedings of the IASTED International Conference, Intelligent, Information Systems, The Bahamas, Dec. 8-10, 1997.

[8] Eberhart RC, Shi Y, Kennedy J. Swarm intelligence: Elsevier; 2001.

[9] Ha Q P, Kwok N M, Nguyen M T, Li J, Samali B, Mitigation of seismic responses on building structures using MR dampers with Lyapunov based control, Structural Control and Health Monitoring, 15(4), (2008), 604-621, DOI 10.1002/stc.218.

[10] Jansen L M, Dyke S J, Semiactive control strategies for MR dampers: comparative study, Journal of Engineering Mechanics, 126(8), (2000), 795-803, DOI 10.1061/(ASCE)0733-9399(2000)126:8(795).

[11] Karami K. and Amini F., Decreasing the damage in smart structures using integrated online DDA/ISMP and semi-active control, Smart Mater. Struct. 21 105017, 2012.

[12] Kuo, B. C. (1994). Automatic Control Systems. Kwok, N. M., Ha, Q. P., and Samali, B. (2007), MR Damper Optimal Placement for Semi- Active Control of Buildings Using an Efficient Multiobjective Binary Genetic Algorithm. The International Association for Automation and Robotics in Construction, Kochi, India.

[13] Lee S H, Minc K W, Lee Y C, Modified sliding mode control using a target derivative of the Lyapunov function, Engineering Structures, 27(1), (2005), 49-59, DOI 10.1016/j.engstruct.2004.08.010.

[14] Nishtani A, Inoue Y, Overview of the application of active/semiactive control to building structures in Japan, Earthquake Engineering and Structural Dynamics, 30(11), (2001), 1565-1574, DOI 10.1002/eqe.81.

[15] Ohtori Y, Christenson RE, Spencer Jr Bf, Dyke SJ, Benchmark control problems for Seismically excited nonlinear buildings, Journal of Engineering Mechanics, 130(4), (2004), 366-385, DOI 10.1061/(ASCE)0733- 9399(2004)130:4(366).

[16] Patrascu, M., Dumitrache, I. Patrut, P., A comparative study for advanced seismic vibration control algorithms; UPB Sci. Bull. series C, 74(4), (2012), 3-16.

[17] Patrascu, M., Ion, A., Evolutionary Modeling of Industrial Plants and Design of PID Controllers: Case Studies and Practical Applications; Nature-inspired computing for control systems, Springer International Publishing, (2016), 73-119.

[18] Santos J. L. et al., A Semi-active Control-oriented Damper Model for an Automotive Suspension6th, IFAC Symposium Advances in Automotive Control, Munich, Germany, July 2010.

[19] Soong T.T., Spencer B., (2002) Supplemental energy dissipation: state of the art and state of the practice, Engineering Structures 243?259.

[20] Spencer Jr B.E, Carlson, J., Sain, M.K et al (1997 June) On the current status of magnetorheological dampers; seismic protection of full-scale structures. In American Control Conference, 1997. Proceedings of the 1997, vol. 1, pp. 58-462.

[21] Spencer B.F., (2008) ?Structural Control in Honor of TakujiKobori?

[22] Udwadia F E, A new approach to stable optimal control of complex nonlinear dynamical systems, Journal of Applied Mechanics, 81(31), (2014), 1-6, DOI 10.1115/1.4024874.

[23] Zaccarian L, Nesic D, Teel A R, Analytical and numerical Lyapunov functions for SISO linear control systems with first order reset elements, International Journal of Robust and Nonlinear control, 21(10), (2011), 1134-1158, DOI 10.1002/rnc.1649.